

## BUILDING DAMAGE ASSESSMENT FOR EARTHQUAKE LOSS ESTIMATION IN TAIWAN

Chin-Hsun YEH<sup>1</sup>, Wen-Yu JEAN<sup>2</sup> And Chin-Hsiung LOH<sup>3</sup>

### SUMMARY

This paper describes procedures of building damage assessment in earthquake loss estimation methodology in Taiwan, and focuses on evaluation of parameters used in the building damage assessment. Since it is neither necessary nor practical to evaluate individual building, building classification and mapping scheme plays an important role. Calculation of site-specific seismic demand and building damage functions (*i.e.*, capacity and fragility curves) are the key features in the building damage assessment. Building capacity is quantified by a pushover curve that describes the nonlinear force-displacement relationship of buildings under monotonic static loads. Building seismic demand considers the effects of hysteretic damping and system degradation due to inelastic structural response. Given definitions of damage states, a set of fragility curves can be established to obtain exceeding probabilities of various damage states given seismic demand and/or system response. A code procedure was proposed to estimate mean capacity spectra of model building types. For calibration purposes, prototype buildings were designed according to the current seismic code used in Taiwan, and static pushover analyses were carried out to determine nonlinear force-displacement relationships. Nonlinear dynamic analyses were also carried out to find mean maximum responses, such as roof displacement, inter-story drift ratio, base shear coefficient, *etc.*, of the prototype buildings. Statistical estimates were obtained to establish fragility curves of the prototype buildings.

### INTRODUCTION

Earthquake loss estimation methodology, integrated with geographic information system (GIS) and designed to run on personal computers, has been developed in the United States and referred as HAZUS [RMS, 1997]. Essentially, Haz-Taiwan follows the approach used in HAZUS. But, to accommodate special environment and engineering practices in Taiwan, minor modifications in analysis models and parameters have been made [Yeh *et al.*, 1999]. As shown in Figure 1, the framework of methodology is mainly composed of input databases, analysis modules and application software. The input database consists of inventory data with GIS information, earthquake hazard and geologic data maps, and analysis parameters. The analysis modules take the required inventory data and analysis parameters as inputs, conduct risk assessment and loss estimation for scenario earthquakes based on site-specific earthquake hazard outputs, and output estimates in the result databases. The third part, integrated with commercial GIS software, is the PC-based application software to execute user's requests, to display input/output databases in both tabular and graphical forms, to generate summary reports, *etc.*

Building damage assessment is one of the important issues in earthquake loss estimation. The results are used to estimate amount of debris, degree of casualties, short-term shelter needs, monetary losses, business interruptions, socio-economic impacts, *etc.*, due to building damage. It is neither necessary nor practical to assess individual building damage. Thus, to facilitate estimation of structural/nonstructural damages and the associated economic losses, general building stocks are classified both in terms of their structural systems, or model building types,

<sup>1</sup> National Center for Research on Earthquake Engineering, Taipei, Taiwan, ROC. Email: chyeh@email.ncree.gov.tw

<sup>2</sup> National Center for Research on Earthquake Engineering, Taipei, Taiwan, ROC. Email: chyeh@email.ncree.gov.tw

<sup>3</sup> Department of Civil Engineering, National Taiwan University, Taipei, Taiwan, ROC.

and in terms of their usage, or occupancy classes, respectively [Kircher et al., 1997]. Since structural system is the key factor in assessing structural performance, loss of function and casualties, damage is predicted based on the model building type. On the other hand, building value is primarily a function of its use. Thus, occupancy class plays an important role in determining economic losses.

Classification rules of model building types are based on structural material (wood, steel, reinforced concrete, masonry, *etc.*), lateral force resistance system (moment resisting frame, frame with bracing system, frame with shear wall, *etc.*), and building height. To accommodate different seismic design levels and building codes, each model building type is further divided into four groups, *i.e.*, high-code, moderate-code, low-code and pre-code. The general occupancies are grouped into residential, commercial, industrial, agricultural, nonprofit/membership organizations, government, and education. Specific occupancies are defined on the basis of standard classification scheme of vocations in Taiwan. There are 37 model building types and 31 specific occupancy classes defined in Haz-Taiwan. A mapping scheme is used to relate the 37 model building types and the 31 specific occupancy classes on the basis of floor area. Once building inventory data has been collected for each occupancy class, the total floor area and building count of each model building type can be obtained.

### ESTIMATION OF BUILDING CAPACITY

In view of the uncertainty and ambiguity involved in the building damage assessment, a simple and practical approach to estimate seismic capacity of each model building type is necessary. In Haz-Taiwan, capacity spectrum method is adopted to represent seismic capacity of model building type. It is derived from concepts similar to those of the NEHRP guidelines [FEMA, 1997] and ATC-40 [SSC, 1996].

A building capacity curve, generally known as a pushover curve, is a plot of lateral load resistance as a function of characteristic lateral displacement. It can be derived from a plot of base shear versus roof displacement when the building is subjected to equivalent static forces. To facilitate direct comparison with demand spectrum, the lateral load resistance is converted to spectral acceleration and the characteristic lateral displacement is converted to spectral displacement using modal properties of the buildings.

As shown in Figure 2, when the capacity spectrum method is applied in building damage assessment, the capacity curve is simplified and contains only two control points, *i.e.*, yield capacity and ultimate capacity. Yield capacity represents the lateral load resistance strength of the building before structural system has nonlinear response, taking into accounts the redundancy in design strength, the conservatism in code requirement, and the extra strength of materials. Ultimate capacity represents the maximum strength of the building when the global structural system reaches a full mechanism. A building is typically assumed to deform beyond the ultimate point without loss of stability, but the structural system provides no additional resistance to lateral load. The yield capacity ( $D_y, A_y$ ) and the ultimate capacity ( $D_u, A_u$ ) can be expressed as

$$A_y = C_s \gamma / \alpha_1, \quad D_y = A_y T_e^2 / (2\pi)^2, \quad A_u = \lambda A_y, \quad \text{and} \quad D_u = \lambda \mu D_y, \quad (1)$$

where  $C_s$  is the design base shear coefficient,  $\gamma$  the over-strength factor relating true yield strength to design strength,  $\alpha_1$  the fraction of effective weight in the pushover mode,  $T_e$  the true period of the pushover mode,  $\lambda$  the over-strength factor relating ultimate strength to yield strength, and  $\mu$  the displacement ductility. In HAZUS,  $C_s$  and  $\mu$  depend on the seismic design levels, while the other factors  $T_e, \alpha_1, \gamma$  and  $\lambda$  are assumed to be independent of design level. To convert roof displacement,  $\delta$ , to spectral displacement,  $D$ , the following equation is used,

$$D = \alpha_2 \delta, \quad (2)$$

where  $\alpha_2$  is the fraction of the building height at the point of pushover mode displacement.

#### ***Proposed Code Procedure***

According to the current building code in Taiwan, total base shear  $V$  is calculated by the formula

$$V = \frac{ZIC}{\Omega\alpha_y F_u} W = C_s W, \quad (3)$$

where  $Z$ ,  $I$ ,  $C$  are the seismic zone factor, building importance factor, normalized design spectrum, respectively, and  $F_u$  is the strength reduction factor. It is noted that both  $C$  and  $F_u$  are functions of structural period and site condition. The value of  $F_u$  depends also on the allowable ductility,  $R_a$ , which is reduced from the ductility capacity  $R$  and is defined as  $R_a = (R+1)/2$ . The parameters  $\Omega$  and  $\alpha_y$  are the over-strength factors corresponding to  $\lambda$  and  $\gamma$  in Eq. (1). According to the seismic design code in Taiwan, the typical values of  $\alpha_y$  are 1.2 and 1.5 for steel and reinforced concrete buildings, respectively. They are about the same as those used in HAZUS. However, the value of  $\Omega$  is 1.4, but the value of  $\lambda$  ranges from 2 to 3 in HAZUS. It is also noted that the ductility capacity  $R$  ranges from 1.6 to 4.8, while the displacement ductility  $\mu$  ranges from 4 to 8 in HAZUS. Thus, one of the objectives in this study is to verify the consistency between the code-specified values and the "true" values from numerical analysis.

According to the current design code in Taiwan, equivalent static analysis can be used to design regular building with height less than 50 meters. The equivalent static force applied at story  $i$  can be expressed as

$$F_i = \frac{(V - F_t)w_i h_i}{\sum_{i=1}^N w_i h_i}, \quad (4)$$

where  $F_t = 0.07T_e V$ ,  $T_e$  is the elastic fundamental period,  $w_i$  and  $h_i$  are the total weight and height at story  $i$ , respectively, and  $N$  is the total number of stories. The factors  $\alpha_1$  and  $\alpha_2$  in Eqs. (1) and (2) can be defined as

$$\alpha_1 = \frac{(\eta_1)^2}{\eta_0 \eta_2}, \quad \alpha_2 = \frac{\eta_2}{\eta_1 \phi_{r1}}, \quad (5a)$$

and

$$\eta_0 = \sum_{i=1}^N w_i, \quad \eta_1 = \sum_{i=1}^N w_i \phi_{i1}, \quad \eta_2 = \sum_{i=1}^N w_i \phi_{i1}^2 \quad (5b)$$

where  $\phi_{i1}$ ,  $\phi_{r1}$  are amplitudes of the first mode at level  $i$  and roof, respectively.

### **Nonlinear Pushover Analysis**

To calibrate parameter values obtained by the proposed code procedure, steel moment resisting frames, with 2-, 5- and 12-story height, were designed according to the allowable stress method in Taiwan. Grade A36 structural steel was used for beam members and Grade A50 for column members. Figure 3 shows the plane and the elevation views of the 12-story prototype building. Column sections are changed every three floors according to the construction practice in Taiwan. Table 1 shows some of the design parameters, where  $h_n$  denotes the total height,  $T_c$  and  $T_d$  are the fundamental periods estimated by the code and the dynamic analysis, respectively, and  $C_s$ ,  $\alpha_y$ ,  $\Omega$ , and  $R$  are defined as before. Assume the prototype buildings are located in Taipei basin where  $Z = 0.23$ . The ductility capacity,  $R$ , is assumed to be 4.8. The building importance factor,  $I$ , is assumed to be 1.0.

DRAIN-2DX program [Prakash and Powell, 1994] for frame analysis is used to carry out the nonlinear pushover analysis. The lateral force applied at each floor was proportional to the code specification in Eq. (4). Both beams and columns are modeled as two-dimensional beam-column elements that provide flexural, shear and axial stiffness. The shear and axial deformation are assumed to remain elastic. The moment-curvature relationship is assumed to be bilinear with 2% strain hardening. Second-order  $P-\Delta$  effect is also considered. The yield strength is defined as the base shear when one of the structural members reaches its yield moment. However, since there is no maximum point in the pushover curves for the steel buildings, the ultimate strength is

artificially defined as the base shear when maximum inter-story drift ratio reaches 3%.

Results of the pushover analyses are summarized in Table 2. Capacity spectra for the 12-story prototype building obtained by the proposed code procedure and pushover analysis are shown in Figure 4. It is noted that the strength estimated by the code procedure is too conservative. Further investigation shows that the over-strength factors  $\alpha_y$  and  $\Omega$ , corresponding to  $\gamma$  and  $\lambda$  in Eq. (1), have larger values in pushover analyses as shown in Table 2. To make the results consistent from the two approaches, the product  $\Omega\alpha_y$  should be raised up 30% for the 12-story prototype building and even more for other low-rise buildings.

## ESTIMATION OF BUILDING SEISMIC DEMANDS

Based on location and magnitude of a scenario earthquake and local geological data, ground motion demands are calculated in terms of response spectra and peak ground values (*e.g.*, PGA and PGV). The estimation process follows three steps described below and is schematically shown in Figure 5:

1. Specify attributes of the scenario earthquake including location, depth, magnitude, fault rupture type, *etc.*
2. Determine the ground motion levels for the bedrock using appropriate attenuation laws.
3. Overlay high-resolution geologic data and modify the ground motion demands using site amplification factors based on local site-soil conditions.

Typical response spectrum can not be expressed as a combination of elementary functions. In Haz-Taiwan, a standard response spectrum shape, as shown in Figure 6, is used to characterize the site-specific response spectrum. The standard shape consists of four parts: PGA, constant spectral acceleration region, constant spectral velocity region, and constant spectral displacement region. The constant spectral acceleration region is defined by 5%-damped spectral acceleration at a period of 0.3 second. The constant spectral velocity region has spectral acceleration proportional to  $1/T$  and is anchored to 1-second, 5%-damped spectral acceleration. Attenuation laws and site amplification factors are supplied for PGA, PGV and spectral accelerations at periods  $T = 0.3$  and  $T = 1.0$  second.

Prediction of inelastic seismic demand of buildings under strong ground shaking generally follows two approaches. One is to model buildings as hysteretic systems and consider effects of damping, ductility, energy dissipation, *etc.*, while the other is to modify the existing elastic response spectra according to structural properties as well as responses during strong ground shaking. In Haz-Taiwan, inelastic demand spectrum is obtained by dividing the 5%-damped elastic response spectrum with damping reduction factors [Newmark and Hall, 1982]. Figure 7 illustrates the process of developing an inelastic demand spectrum from the 5%-damped elastic response spectrum distinguishing between domains of constant spectral acceleration and constant spectral velocity.

The damping reduction factors shown in Figure 7 are assumed to be functions of effective damping ratio,  $\beta_{eff}$ , which is defined as the total dissipated energy during peak earthquake response. The effective damping ratio, being the sum of elastic and hysteretic damping ratios, can be expressed as

$$\beta_{eff} = \beta_E + \beta_H = \beta_E + \kappa \left( \frac{A_H}{2\pi DA} \right), \quad (6)$$

where  $D$  and  $A$  represent the peak displacement and acceleration, respectively,  $A_H$  the area enclosed by the hysteresis loop as illustrated in Figure 7,  $\kappa$  a degradation factor that defines the effective percentage of  $A_H$  in energy dissipation. The elastic damping ratios typically are 5% to 10% depending on model building types. The damping reduction factors typically increase for buildings that have reached yield and dissipate hysteretic energy during cyclic response. The value of  $\kappa$  is about 0.6 to 0.9 for ductile systems and 0.5 for non-ductile systems such as unreinforced masonry buildings. Due to system degradation, the value of  $\kappa$  is further decreased as the duration of strong ground shaking becomes longer. Since hysteretic damping and inelastic structural response are mutual dependent, iteration process is generally required to obtain the final results.

## ESTIMATION OF BUILDING DAMAGES

Mean maximum response of a model building type under a scenario earthquake is estimated by the intersection of the inelastic demand spectrum and the associated capacity curve. Figure 8 shows the intersections of three demand spectra representing weak, medium and strong ground shaking levels, and two building capacity curves representing a weaker and a stronger construction, respectively. As shown in the figure, the stronger and stiffer construction displaces less than the weaker and more flexible construction for the same level of spectral demand. Less damage is expected to the structural system and drift-sensitive nonstructural components. However, since the stronger construction will shake at higher acceleration levels, more damage is expected to acceleration-sensitive nonstructural components and building contents.

To better estimate different types of losses, Haz-Taiwan separately predict damage to the structural system, drift-sensitive and acceleration-sensitive nonstructural components. Damage states are also defined separately for structural system and nonstructural components of a building. Although actual building damage varies as a continuous function of earthquake demand and structural response, four discrete damage states, *i.e.*, slight, moderate, extensive and complete damage states are used to describe the building damage levels and to provide information regarding the building's physical conditions.

Fragility curves are often used to estimate probability of reaching or exceeding various damage states, given estimates of seismic demands or structural responses. The fragility curve is often modeled as a lognormal function and is defined by a median value,  $\bar{s}_d$ , corresponding to the mean threshold of associated damage-state, and by a logarithmic standard deviation,  $\beta$ . Thus, the conditional probability of being in, or exceeding, a particular damage state,  $d_i$ , given seismic demand,  $s_d$ , is defined by

$$P(DS \geq d_i | s_d) = \Phi \left[ \frac{1}{\beta} \ln \left( \frac{s_d}{\bar{s}_d} \right) \right], \quad (7)$$

where  $\Phi(\cdot)$  is the standard normal distribution function.

As an example, if PGA is used in constructing a fragility curve, the fragility curves of a particular building can be constructed by following procedures stated below:

- 1) Select earthquake ground motion model with hazard consistent PGA distribution.
- 2) Define limiting states for discrete damage levels.
- 3) Analyze the building response using inelastic dynamic analysis.
- 4) Conduct risk analysis to obtain the probability of exceeding various limiting states.

In this study, a set of 34 records from Taiwan earthquake database was used as the inputs in nonlinear dynamic analysis. Peak ground accelerations were normalized to different excitation levels. The statistical estimates of structural response, *e.g.*, roof displacement, dissipated energy, inter-story shear and drift ratio, *etc.*, were calculated. If the limiting states for discrete damage levels were defined by the roof displacement reaching 10 cm, 20 cm, 30 cm, and 50 cm, respectively, Figure 9 shows the corresponding fragility curves of the 12-story prototype building. The smooth curves shown in the figure are log-normal functions which were best-fit to the sample points.

Intuitively, it is more adequate to specify the limiting states by using inter-story drift ratios. However, the distribution of inter-story drift ratios is often not uniform and depends on the type of structural systems, vertical distribution of stiffness and strength, *etc.*, of individual building, as shown in Figure 10. In Haz-Taiwan, spectral displacement is used for estimating structural damage and for constructing fragility curves. The spectral displacement is derived from the roof drift ratio as in Eq. (2) and is estimated by the intersection of nonlinear seismic demand and building capacity curve in acceleration-displacement response spectrum. The damage assessment process for structural systems and nonstructural components is shown schematically in Figure 11. To consider actual distribution of inter-story drift ratios, the median value of roof drift ratio has been implicitly reduced for high-rise buildings. The discrete probability in each damage state is obtained by subtracting adjacent fragility curves. Estimation of mean thresholds of damage states may be based on experience and/or capacity curves for model building types.

## CONCLUSIONS

The procedure of building damage assessment in Haz-Taiwan was presented. Although dispersions of seismic demand, building capacity and fragility curves have not been discussed here, they are very important topics and will be investigated in the future. Comparison of building capacity curves obtained by the proposed code procedure and pushover analysis shows that the proposed code procedure can be adopted to estimate the mean capacity spectra of model building types. However, due to conservatism in code requirement, some modifications in code-specified parameter values should be made. The amount of modification in each parameter, such as  $T_c$ ,  $\alpha_y$ ,  $\Omega$ ,  $\alpha_1$  and  $\alpha_2$ , depends on different structural system, material and height, *i.e.*, model building type. The pushover analysis shows that a larger value of  $\Omega\alpha_y$  should be used for steel moment resisting frames. The "true" over-strength factors for low-rise steel moment resisting frames are larger than those of high-rise ones.

## ACKNOWLEDGEMENT

This study was supported by the National Science Council under Grant No. NSC 87-2621-9-319-001.

## REFERENCE

- Federal Emergency Management Agency (FEMA) (1997), *NEHRP Guidelines for the Seismic Rehabilitation of Buildings*, Washington, D.C., USA.
- Kircher, C. A., Nassar, A. A., Kustu, O. and Holmes, W. T. (1997), "Development of building damage functions for earthquake loss estimation", *Earthquake Spectrum*, 13, 4, pp 663-682.
- Newmark, N. M. and Hall, W. J. (1982), *Earthquake Spectra and Design*, Earthquake Engineering Research Institute Monograph.
- Prakash, V. and Powell, G. H. (1993), *DRAIN-2DX: Base Program User Guide*, Version 1.10, , Department of Civil Engineering, University of California, Berkeley, CA.
- Risk Management Solutions, Inc. (1997), *Earthquake Loss Estimation Methodology - HAZUS97 Technical Manual*, National Institute of Building Sciences, Washington, D.C.
- Seismic Safety Commission (SSC) 1996, *Seismic Evaluation and Retrofit of Concrete Buildings*, SSC Report No. 96-01, Sacramento, CA, USA.
- Yeh, C. H., Lee, C. Y. and Loh, C. H. (1999), "Framework of earthquake loss estimation method in Taiwan", *Proceedings 1999 Workshop on Disaster Prevention/Management & Green Technology*, Foster City, CA, USA.

**Table 1: Design parameters for the steel prototype buildings.**

Prototypes	$h_n$ (m)	$T_c$ (sec)	$T_d$ (sec)	$C_s$	$\alpha_y$	$\Omega$	$R$
ST12 (x)	46.8	1.52	1.86	0.084	1.20	1.40	4.8
ST5 (x)	19.5	0.79	1.14	0.107	1.20	1.40	4.8
ST2 (x)	7.8	0.40	0.57	0.125	1.20	1.40	4.8

**Table 2: Results of pushover analysis for prototype buildings.**

Prototypes	$C_y$	$C_u$	$D_y$	$D_u$	$\gamma$	$\lambda$	$\gamma\lambda/(\alpha_y\Omega)$	$\alpha_1$	$\alpha_2$	$\mu$
ST12 (x)	0.113	0.188	0.202	0.909	1.35	1.66	1.33	0.761	0.727	4.50
ST12 (y)	0.103	0.181	0.204	1.108	1.23	1.76	1.29	0.754	0.708	5.43
ST5 (x)	0.130	0.293	0.065	0.282	1.21	2.25	1.62	0.774	0.747	4.34
ST5 (y)	0.163	0.288	0.092	0.511	1.52	1.77	1.60	0.773	0.742	5.55
ST2 (x)	0.269	0.529	0.033	0.217	2.15	1.97	2.52	0.858	0.843	6.58
ST2 (y)	0.245	0.459	0.038	0.147	1.96	1.87	2.18	0.857	0.830	3.87

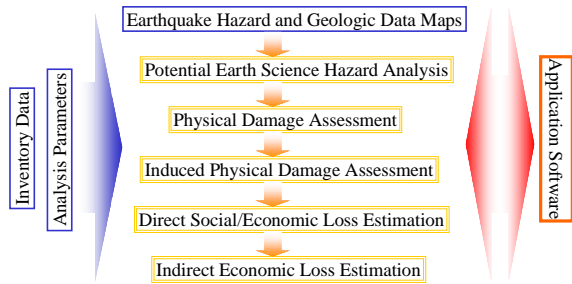


Fig 1: Framework of methodology in Haz-Taiwan.

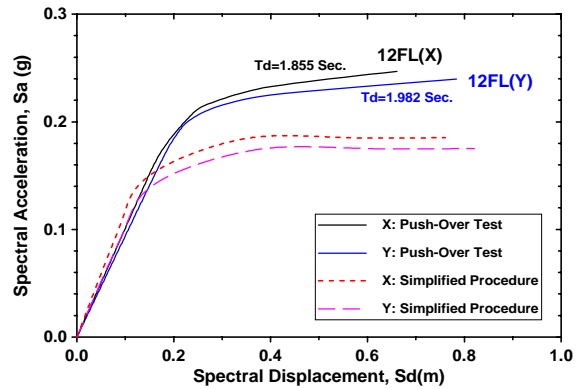


Fig 4: Comparison of capacity spectra using the proposed code procedure and pushover analysis

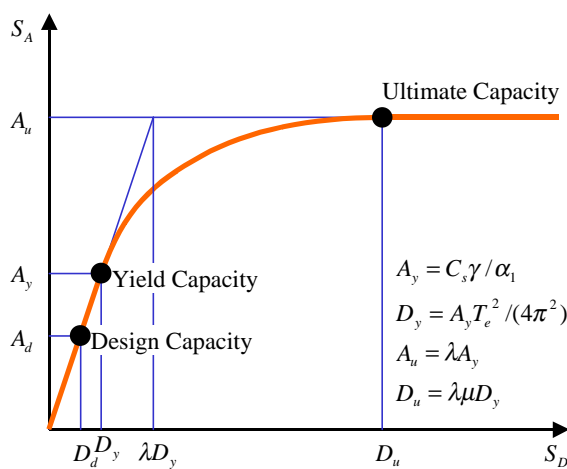


Fig 2: Definitions of yield capacity and ultimate capacity of a building.

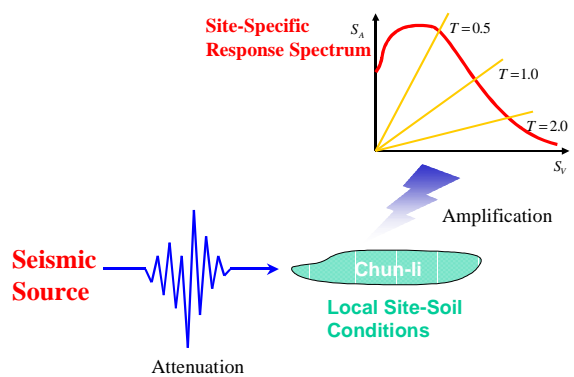


Fig 5: Calculation of ground shaking in deterministic approach.

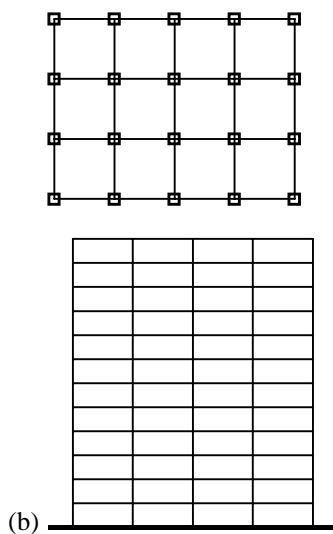


Fig 3: (a) Plane and (b) elevation views of 12-story steel MRF prototype building.

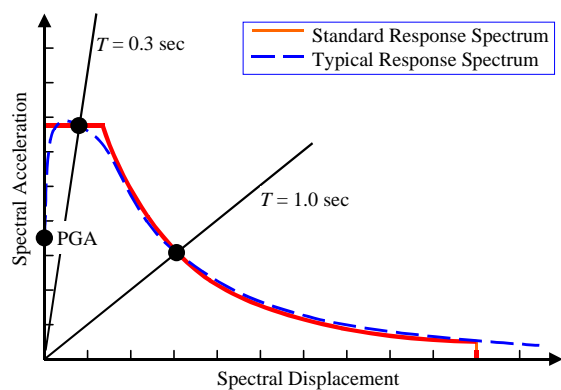


Fig 6: Standard shape of response spectrum

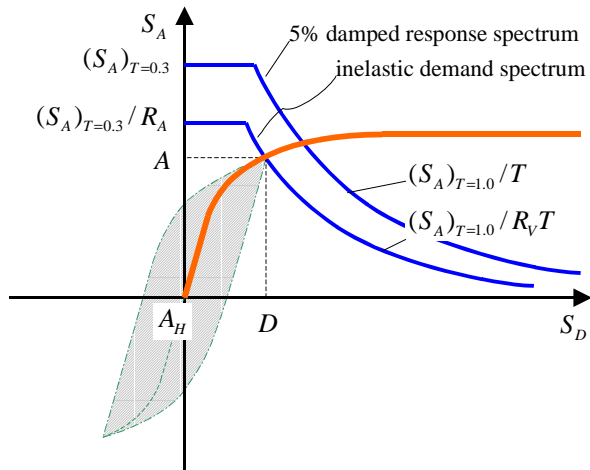


Fig 7: Modification of inelastic demand spectrum by damping reduction factors

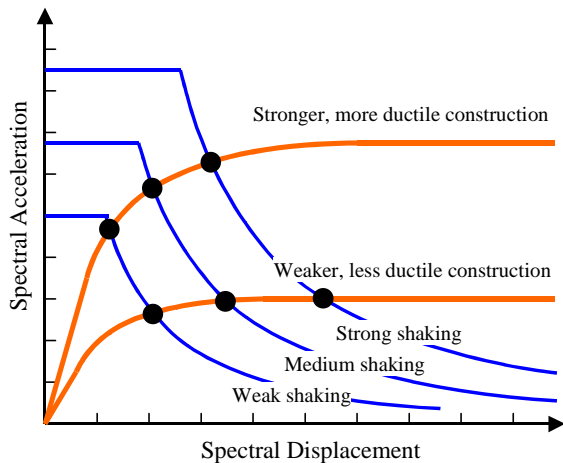


Fig 8: Intersection points represent mean maximum response of buildings under different levels of ground shaking

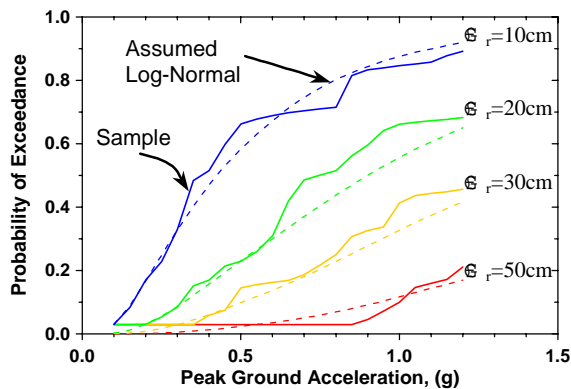


Fig 9: Fragility curves in terms of PGA levels for 12-story prototype building.

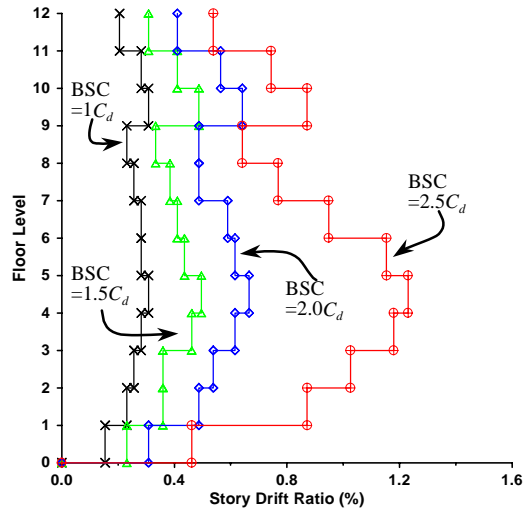


Fig 10: Distribution of inter-story drift ratios for 12-story prototype building under static pushover analysis.

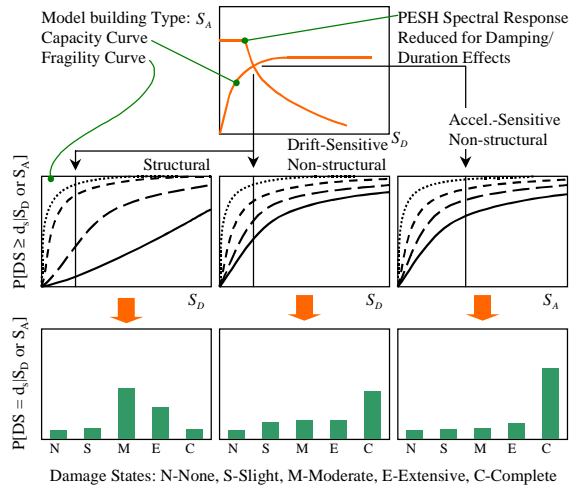


Fig 11: Procedures of building damage assessment